Monatsh Chem (2014) 145:435–445
DOI 10.1007/s00706-013-1122-4

ORIGINAL PAPER

Synthesis and characterization of novel bis(diphenylphosphino)-oxalyl and (substituted) malonyl dihydrazones: P,N,N,P-tetradentate complexes of an oxalyl derivative with Cu(II), Pd(II), and Mn(II)

Mohamed Shaker S. Adam · Ahmad Desoky M. Mohamad · Omar M. El-Hady

Received: 17 January 2013 / Accepted: 13 November 2013 / Published online: 14 December 2013

Abstract Novel ligands of bis(diphenylphosphino)-oxalyl, malonyl, and methyl- and ethyl-malonyl dihydrazones were synthesized by condensation of oxalyl, malonyl, methyl-malonyl, and ethyl-malonyl dihydrazide with *o*-(diphenylphosphino)benzaldehyde in different conditions. The dihydrazones exhibit three different tautomeric structures detected by NMR and IR spectra. The ^{31}P NMR spectrum demonstrates four different singlet signals, i.e., chemical shifts, of the three respective tautomers. Complexes of the oxalyl ligand with Pd^{2+}, Cu^{2+}, and Mn^{2+} ions are formed in 1:1 molar ratio. Their structures were characterized by IR, NMR, EPR, MS, EA, and TGA, in which the oxalyl ligand acts as a neutral P,N,N,P-tetradentate chelate. The pH stability of the complexes is in the region of ca. 4.5–7.5 and their activation energy was calculated from the conductivity measurements.

Keywords Aldehyde · Tautomerism · Carbonyl–enols · Metal(II) complexes

Introduction

Synthesis, structural investigation, and reactions of transition metal complexes with N-donor ligands, e.g., Schiff base hydrazones, have gained attention in research because of their biological activities [1–3]. Acyl-, aroyl-, and phthaloyldihydrazones (di-Schiff bases) are polyfunctional N,O,O,N-type ligands [4, 5] which form mono-, di-, and polynuclear complexes involving ligand bridging and oxo-bridging [6, 7]. Metal complexes of dihydrazones are of interest in studies related to homogeneous catalysis, multi-electron-transfer processes, and oxygen-atom-transfer reactions [8–10].

Recently, extensive fundamental research into phosphine chemistry has highlighted the synthesis of new series of phosphine ligands with alternative donor atoms besides phosphorus, e.g., N and/or O atoms [11–15] (the electronic asymmetry or electronic differentiation and hemilability [16–20]). One group of hemilabile phosphine ligands involving the combination of phosphorus and other donor heteroatoms as chelate agents for complexation [21] are of particular interest because of their applications in catalysis. Such ligands can display quite different coordination modes as multidentate ligands [22–43]. Moreover, phosphine–Schiff base chelates of P,N and P,N,O types form fairly effective catalysts with transition metals, e.g., Cu(I) [44, 45] and Pd(II) [46, 47]. They are highly enantioselective in various reactions, e.g., hydroboration, hydrosilylation, epoxidation, aziridination of olefins, the Henry reaction, and allylic substitutions [46, 47]. Morris et al. developed the synthesis and applications of a new series of P,N,N,P-tetradentate ligands complexed to iron(II) as precatalysts for asymmetric transfer hydrogenation of ketones or carbonyl compounds [22–35].

Schiff bases have been extensively studied as they possess many interesting features, including photochromic and thermochromic properties [48], proton transfer tautomeric equilibria [49], and suitability for analytical applications [50]. Some Schiff bases are unstable in solution and involved in various equilibria like carbonyl–enol or in ring–chain tautomeric interconversion, hydrolysis, or

---

Electronic supplementary material The online version of this article (doi:10.1007/s00706-013-1122-4) contains supplementary material, which is available to authorized users.

M. S. S. Adam (✉) · A. D. M. Mohamad · O. M. El-Hady
Department of Chemistry, Faculty of Science, Sohag University, Sohâg 82534, Egypt
e-mail: shakeradam61@yahoo.com

Scheme 1

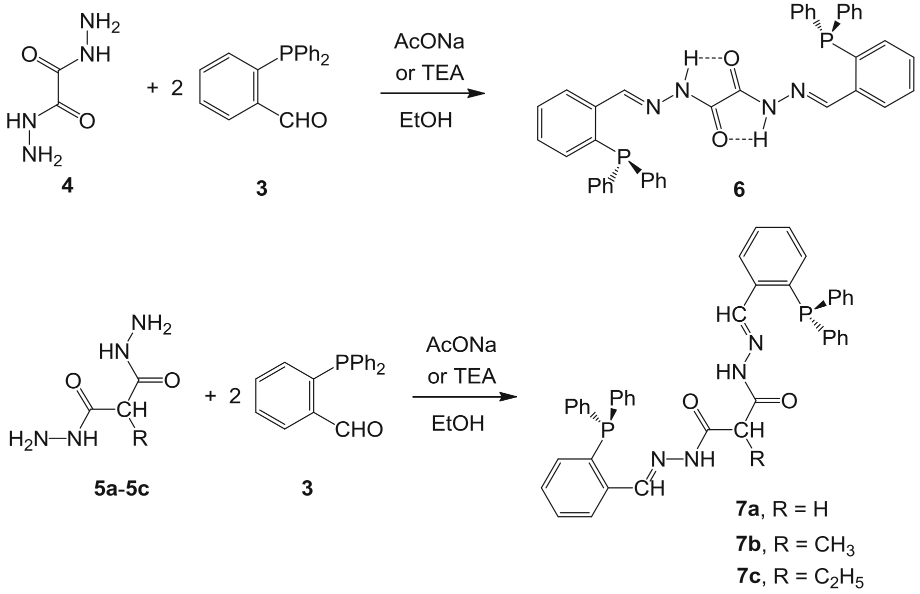

some others [51]. Therefore, their successful application requires a detailed study of their characteristics, i.e., the electronic and structural properties of the ligands play an important role in their catalytic properties [52].

To the best of our knowledge, there is no report on the synthesis and characterization of *o*-(diphenylphosphino)benzaldehyde dihydrazones, despite the importance of such polydentate ligands, e.g., in catalysis. For this reason, we present here the synthesis and characterization of novel bis(diphenylphosphino)dihydrazones via condensation of oxalyl, malonyl, and substituted malonyl dihydrazides with *o*-(diphenylphosphino)benzaldehyde. We studied their spectroscopic characteristics and tautomeric properties. Moreover, the coordination behavior of the oxalyl hydrazone ligand with Cu(II), Pd(II), and Mn(II) was also studied as representative compounds.

Results and discussion

*Synthesis of bis(diphenylphosphino)dihydrazones **6** and **7a–7c***

The synthesis of tetra- or hexadentate novel P,N and/or O ligands **6** and **7a–7c** started in situ by standard condensation of oxalyl, malonyl, methyl-malonyl, and ethyl-malonyl dihydrazides (**4** and **5a–5c**) with 2 equivalents of *o*-(diphenylphosphino)benzaldehyde (**3**) under different conditions. *o*-(Diphenylphosphino)benzaldehyde (**3**) was prepared according to a reported procedure [53]. Thus, bromine–lithium exchange of *o*-dibromobenzene (**1**) with *n*-butyl lithium at −100 °C followed by treatment with diphenylchlorophosphine afforded *o*-(diphenylphosphino)bromobenzene (**2**) in 81 % yield. The latter underwent a second bromine–lithium exchange with *n*-butyl lithium at −78 °C followed by addition of freshly dried DMF at −78 °C and workup with HCl (3.0 M) at room temperature to give product **3** in 72 % yield after purification by column chromatography [53]. Oxalyl and malonyl dihydrazides **4** and **5a–5c** were synthesized by using published methods [48, 54], by mixing diethyl oxalate and diethyl malonates with excess hydrazine monohydrate in ethanol at room temperature for the oxalyl dihydrazide **4** and under reflux for the malonyl dihydrazides **5a–5c**.

Table 1 Yield of products **6** and **7a–7c**

Entry	Catalyst/media	Yield/%[a]			
		6	**7a**	**7b**	**7c**
1		63	50	42	38
2	AcONa or TEA	91	93	85	75
3	Dilute HCl (pH 4–5)	52	41	40	28

[a] Yield reported after purification by column chromatography

Condensation of **4** or **5a–5c** (1 molar equivalent) with **3** (2 molar equivalents) under reflux in the absence and presence of different reagents was attempted in ethanol (Scheme 1). White solid precipitates of **6** and **7a–7c** were collected and purified by column chromatography (Table 1).

The yields of **6** and **7a–7c** were low in the absence of anhydrous sodium acetate or TEA (Table 1, entry 1), whereas in their presence the yields were the highest (entry

2). Other attempts to improve the yield of the current ligands were tested in various conditions (highly aqueous basic media, highly aqueous acidic media, piperidine; discussed in the Supplementary Material), e.g., diluted HCl (Table 1, entry 3).

It was observed that the substituent (R = H, Me, Et) in **5a**–**5c** has a remarkable impact on the yield of **7a**–**7c**. The yield of **7** was the highest when R = H (**7a**) and the lowest when R = Et (**7c**) (Table 1). Clearly, the electron-donating nature of the alkyl group tends to reduce the reactivity of **5a**–**5c** towards condensation with **3**.

*Characterization and tautomeric behavior of **6** and **7a**–**7c***

Many reports highlighted the isomerization of Schiff base dihydrazone ligands (*staggered*–*anti cis* isomers) [4, 5, 55]; however, we focused here only on the tautomeric behavior evidenced by the NMR spectral results, especially the ^{31}P NMR spectra. The structures of **6** and **7a**–**7c** were confirmed by various spectroscopic techniques including IR, ^{1}H, ^{13}C, and ^{31}P NMR, and low and high resolution mass spectroscopy. Attempts to produce single crystals of **6** and **7a**–**7c** were not successful. Ligands **6** and **7a**–**7c** are very sparingly soluble in polar solvents, e.g., methanol, acetone, and acetonitrile, and highly soluble in more hydrophobic solvents, e.g., chloroform and diethyl ether.

Ligands **6** and **7a**–**7c** are air stable in the solid state but in solution they underwent oxidation after 3 days maximum. The diphenylphosphino group was oxidized in air to a diphenylphosphine oxide group. The structures of the oxidized products were confirmed by the shift of the phosphorus signal in the ^{31}P NMR spectra, namely from -16.0 ppm in **7b** and and -16.6 ppm in **7c** (in $CDCl_3$) to 31.0 and 25.6 ppm, respectively, after oxidation in air.

*NMR and IR spectra of **6** and **7a**–**7c***

NMR spectra of **6** and **7a**–**7c** were recorded in $CDCl_3$ and DMSO-d_6. The NMR spectra showed very little evidence for the tautomeric behavior of **6** which is consistent with reported salicylaldehyde benzoylhydrazone ligands and their metal complexes [48–51, 54]. Dienol, carbonyl–enol, and dicarbonyl forms were observed by NMR spectroscopy. The absence of any tautomeric behavior in **6** could be attributed to the intramolecular hydrogen bonding between the NH protons and C=O oxygens (Scheme 1) which stabilizes the dicarbonyl form. The intramolecular hydrogen bonds in **6** could be detected by the downfield shift of the NH protons in the ^{1}H NMR spectra ($\delta = 10.2$ ppm) [56]. Furthermore, the IR spectra of **6** showed no absorption bands for –OH groups and showed a set of bands at 3,454, 1,687, and 1,505 cm^{-1} due to vibrations of amide NH, C=O, and C=N, respectively. The ^{31}P NMR spectra of **6** showed a signal at -11.6 ppm (Fig. 1).

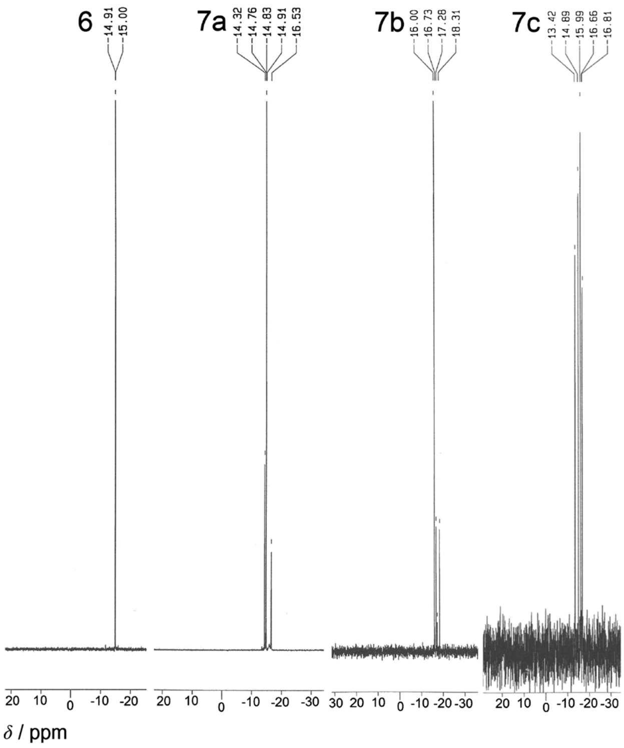

Fig. 1 ^{31}P NMR spectral signals of the tautomers of compounds **6** and **7a**–**7c**

On the other hand, **7a**–**7c** have three tautomeric structures which coexist in solution (Scheme 2) as clearly observed by NMR and IR. The ^{1}H NMR spectrum of **7a** showed that the methylene protons of the malonyl scaffold resonated as three singlet signals at 3.97, 3.80, and 3.31 ppm as a result of three tautomers. The NH proton appears as two broad signals at 10.58 and 10.70 ppm due to the dicarbonyl and carbonyl–enol forms (see Supplementary Material). The strong downfield shifted NH proton could be attributed to the intermolecular hydrogen bonds. In the ^{13}C NMR spectrum of **7a**, the methylene carbon resonated as three singlet signals at 29.7, 38.4, and 39.3 ppm due to the three tautomers (dienol, carbonyl–enol, and dicarbonyl forms). The ^{1}H NMR spectra of **7b** reports two doublet signals of the methyl group at 1.46 and 1.61 ppm and two quaternary signals of the CH-methylene at 4.23 and 4.55 ppm. Moreover, for **7c**, the ^{1}H NMR spectra recorded two triplets for the methyl protons of the ethyl derivative which resonated at 0.94 and 1.07 ppm and two triplets for the CH proton of the malonyl scaffold at 4.24 and 4.65 ppm (Fig. 2).

The IR spectra of **7a** and **7b** gave broad absorption bands at 3,463 and 3,460 cm^{-1}, respectively, which originated from the –OH vibration in the dienol and carbonyl–enol forms. The tautomeric absorption band of the NH

Scheme 2

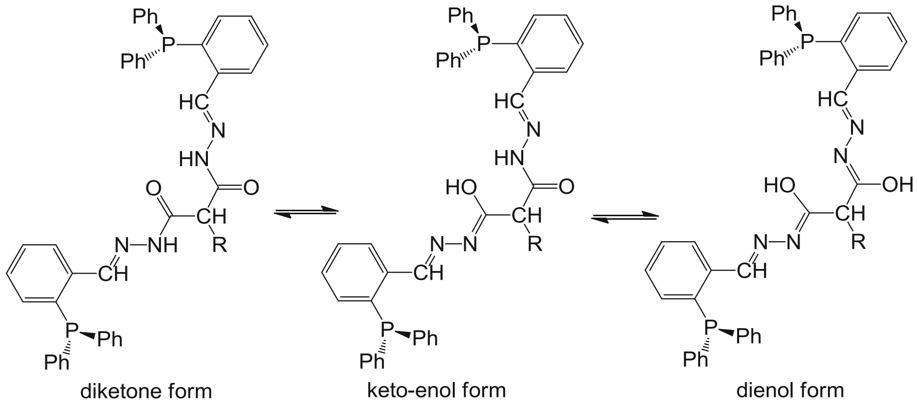

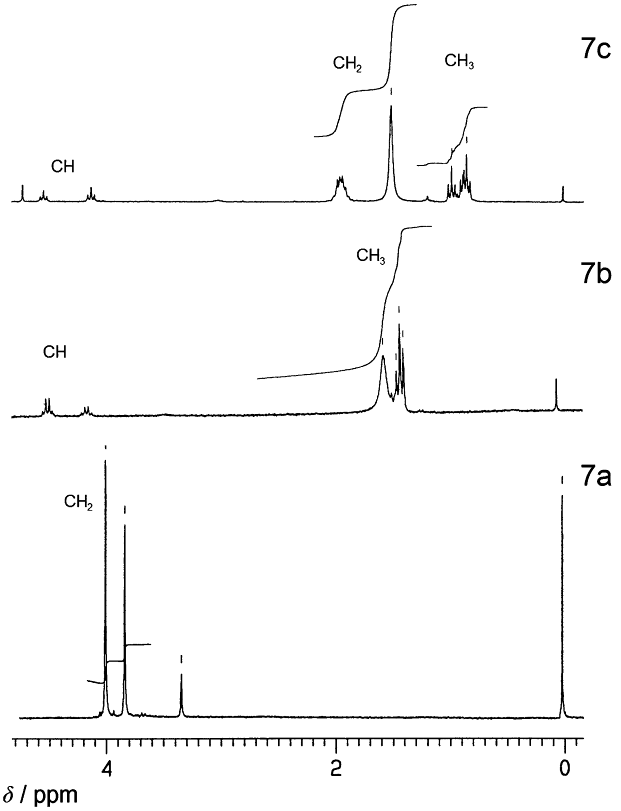

Fig. 2 Expansion of the ^{1}H NMR spectra (0–5 ppm) of the CHR group (R = H, Me, and Et) of compounds **7a**–**7c**

group of the secondary amide group appears conspicuous at 3,421 cm^{-1} for **6a**, whereas it was a broad band for **7b**. In the IR spectrum of **7a**, the C=O and C=N amido groups appear as an overlapped broad band at 1,660 cm^{-1} and the C=N tautomeric group appears at 1,390 cm^{-1}. The characteristic C=O appears at 1,680 cm^{-1} for **7b** and the C=N bands of the amide tautomeric structure appear at 1,560 and 1,452 cm^{-1}. The characteristic C=N stretching absorption band appears within the 1,620–1,640 cm^{-1} region for Schiff bases [57], whereas these appear at 1,687, 1,571, and 1,560 cm^{-1} for **6** and **7a** and **7b**, respectively, owing to the impact of the neighboring amido (NH–C=O) group and the tautomerism.

The ratio of the three coexisting tautomers in **7a**–**7c** was determined by their integration factors in the ^{1}H NMR spectra. For example, in **7a**, the ratio of dienol to carbonyl–enol to dicarbonyl was 8:1:2. In particular, the most abundant and stable tautomer in solution in different polar solvents is the dienol form as observed previously [55]. The intermolecular hydrogen bonding in the dienol tautomer between the hydrogen atom of the –OH group and the nitrogen atom of the CH=N group of another molecule could be the reason for the higher stability of the dienol form than the other forms. The intermolecular hydrogen bonding in the dienol reduces the steric repulsion between the carbonyl groups especially in the less polar solvents [58]. The ^{31}P NMR spectra showed four signals for the three aforementioned tautomers (Fig. 1).

The electronic spectral bands for **6** and **7a**–**7c** are summarized in Table 2, along with their characteristic molar extinction coefficients. All ligands exhibit two bands within the region of 220–243 and 274–306 nm which arise due to π → π* and *n* → π* electronic transitions within dihydrazone, respectively [48].

Theoretical calculations of ***6*** *and* ***7a–7c***

Semiempirical calculations were carried out using the AM1 method with the MOPAC 6.0 program as an experiential study [59]. Energy minimum geometries were found by minimizing the energy, with respect to all geometrical coordinates without any symmetry constraints [60]. Ligand **7a** assembled in a dense, hydrogen-bonded network with all six geometrically possible hydrogen bonds realized. All hydrogen bonds have a length of 2.94 ± 0.2 Å. Calculated heats of formation of the optimized structures of both compounds revealed that **7a** is more stable than **6** (see Supplementary Material).

*Synthesis of Cu(II), Pd(II), and Mn(II) acetate complexes **8**, **9**, and **10***

Ligand **6** acts as a tetradentate chelate, whereas ligands **7a**–**7c** may act as hexadentate ligands as dibasic anions in the dienolic forms and as tetrabasic moieties in the dicarbonyl forms under suitable conditions [61] that will be studied and presented in future work. We tested the coordination chemical behavior of **6** only as a model towards Cu(II), Pd(II), and Mn(II) ions. The novel complexes were synthesized by mixing **6** with Cu(II), Pd(II), and Mn(II) acetate in equimolar ratio in methanol at room temperature. The general formula of the current complexes is [ML](OAc)$_2$S, where L is **6** and S is the solvent, particularly H_2O or MeOH (Scheme 3).

The stoichiometry of the current complexes was determined by the widely used spectrophotometric continuous variation method [62] in which the molar ratios of the individual components of the tested complexes varied continuously in solution, whereas the total concentration remained constant. The continuous variation plots (see Supplementary Material) reveal maximum absorbance values at λ_{max} corresponding to molar ratios of 0.98–1.01 of the oxalyl ligand in the studied complexes. This suggests that the metal ion formed a 1:1 complex with **6** (Scheme 3). In particular, **6** coordinated to the central metal ion through the α-nitrogen of the diimino group and the two phosphorus atoms of the bis(diphenylphosphino) group. Complex **8** is olive-brown, whereas **9** and **10** are pale brown. The complexes are air stable in the solid state and also in solution (in polar solvents, e.g., MeOH, EtOH, and MeCN).

Table 2 Electronic spectra and the activation energy for compounds **6**–**10**

Product	Electronic spectra[a]			Activation energy[b] $E \times 10^{-3}$/kJ mol^{-1}
	λ_{max}/nm	10^4 ε_{max}/dm^3 mol^{-1} cm^{-1}	Assignment	
6	222	6.04	$\pi \rightarrow \pi^*$	
	274	1.11	$n \rightarrow \pi^*$	
7a	234	7.10	$\pi \rightarrow \pi^*$	
	296 br	3.70	$n \rightarrow \pi^*$	
7b	236	5.23	$\pi \rightarrow \pi^*$	
	300 br	3.45	$n \rightarrow \pi^*$	
7c	243	6.37	$\pi \rightarrow \pi^*$	
	306 br	3.21	$n \rightarrow \pi^*$	
8	221	5.68	$\pi \rightarrow \pi^*$	2.14
	312	2.42	LMCT	
	351 br	4.91	d–d	
9	229	7.18	$\pi \rightarrow \pi^*$	1.35
	317	2.57	LMCT	
	445 br	5.95	d–d	
10	222	6.61	$\pi \rightarrow \pi^*$	1.57
	320	2.37	LMCT	
	425 br	5.34	d–d	

LMCT ligand–metal charge transfer band

[a] Electronic spectra were recorded in methanol

[b] Activation energies were measured for each complex at a concentration of 2.0×10^{-5} mol dm^{-3} at 298 K

*Characterization of complexes **8**–**10***

The complexes **8**–**10** were characterized by IR, ^{1}H NMR, ^{13}C NMR, ^{31}P NMR, EPR, MS, and UV–Vis spectra, and EA. The electronic spectral data of **8**–**10** and **6** are summarized in Table 2. The elemental analyses were in good agreement with the calculated values after purification. The complexes are single species as confirmed by TLC tests. The methanolic solutions of **8**–**10** show uniform spots on a TLC plate covered with silica gel and developed using a mixture of acetone and methanol (2:1).

*IR, NMR, and EPR spectra of complexes **8**–**10***

The IR spectra of **8**–**10** illustrated that most bands are almost in the same position as those of the uncoordinated ligand **6** but considerably reduced in their intensity. No observed changes were seen for the NH and C=O bands after complexation with Cu(II), Pd(II), or Mn(II) ions. The bands of the HC=N group coordinated to the central metal ion show a strong shift of its stretching vibrations from 1,505 cm^{-1} in **6** to 1,636, 1,685, and 1,564 cm^{-1} in **8**–**10**, respectively.

Scheme 3

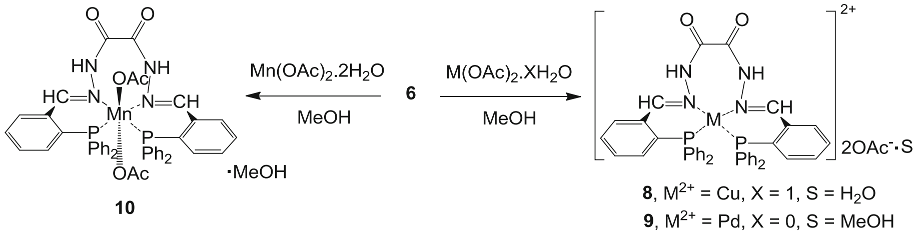

Complexes **8** and **10** are paramagnetic, whereas **9** is diamagnetic. In the ^{1}H NMR spectra of **9**, the proton resonances of the methyl group of the acetate ion and of the coordinated methanol appear at 1.84 and 5.97 ppm as singlets, respectively. A little downfield shift of the HC=N proton resonance is observed from 8.99 (in **6**) to 9.01 ppm (in **9**) which appears as a doublet with higher coupling from 5.7 (in **6**) to 11.2 Hz (in **9**) which is attributable to the coordination through the nitrogen atom to the Pd^{2+} ion. In the ^{13}C NMR spectra, the acetate ion shows two signals at 22.0 and 175.5 ppm corresponding to CH_3 and C=O carbons, respectively. The other ^{13}C NMR spectral signals do not have observed shift after complexation.

The EPR spectra of the Cu(II) complex were recorded in methanol at 115 K (Fig. 3). The X-band EPR spectra of the Cu(II) complex, particularly **8**, show one intense absorption band in the high field region. This band is isotropic owing to the tumbling motion of the molecules. However, this complex in the frozen state shows five well-resolved peaks in the low field region. It exhibits anisotropic signals with g values ($g_{\|} = 2.066$ and $g_{\perp} = 2.009$) which are characteristic of axial symmetry [63]. Since the $g_{\perp}$ and $g_{\|}$ values are closer to 2 and $g_{\|} > g_{\perp}$, this suggests a square-planar geometry around the Cu(II) ion corresponding to elongation along the fourfold symmetry *Z*-axis [64, 65]. In addition, exchange coupling interaction between two Cu(II) ions of two complex cations was explained by Hathaway's expression $G = (g_{\|} - 2)/(g_{\perp} - 2)$. The G value of 7.33 indicated negligible exchange interaction coupling of Cu–Cu within two complex cations [66, 67], see Fig. 3. The EPR spectrum of the Mn(II) complex **10** was measured in DMSO as a polycrystalline sample at 311 K (Fig. 4), giving two main signals with $g_{\|} = 1.887$ and $g_{\perp} = 2.123$. The polycrystalline samples gave one broad isotropic signal centered approximately at around the free electron g value (2.0023). The complex gave an EPR spectrum containing six lines due to hyperfine interaction [68–70] between the unpaired electrons and the ^{55}Mn nucleus ($I = 5/2$). The nuclear magnetic quantum numbers *MI* corresponding to the lines are −5/2, −3/2, −1/2, +1/2, +3/2, and +5/2 from low to high field (Fig. 4).

*Electronic spectra of complexes **8–10***

The electronic absorption spectra are often very helpful in the evaluation of results furnished by other methods of structural investigation. Moreover, the electronic spectral measurements were used to assign the stereochemistries of metal ions in the complexes on the basis of the positions and number of d ↔ d transition peaks.

The electronic spectra of the synthesized complexes compared to their corresponding ligand **6** show three bands in the region 222–229 ($\pi \rightarrow \pi^*$), 312–320 (LMCT), and 351–425 nm (d ↔ d) in methanol (Table 2). The appearance of bands in the regions 221–229 and 312–320 nm in the complexes suggests that the ligand (222 and 274 nm in **6**, respectively) undergoes splitting and shows blue shift as well as red shift. This feature associated with the ligand indicates an effect of complexation on the ligand. The complexes show another strong broad band in the region of 351–425 nm in the visible region, cf. Table 2. Since **6** is not expected to be chromophoric in the visible region, these bands have been assigned as ligand–metal charge transfer (LMCT) transitions on the basis of their high intensity [70]. They may be associated, most probably, with a ligand-to-metal charge transfer originating from an electronic excitation from the HOMO of bis(diphenylphosphino) to the LUMO of the complexes as reported before [48]. Also, the broad bands appearing as moderately intense peaks in the region 351–445 nm of the complexes

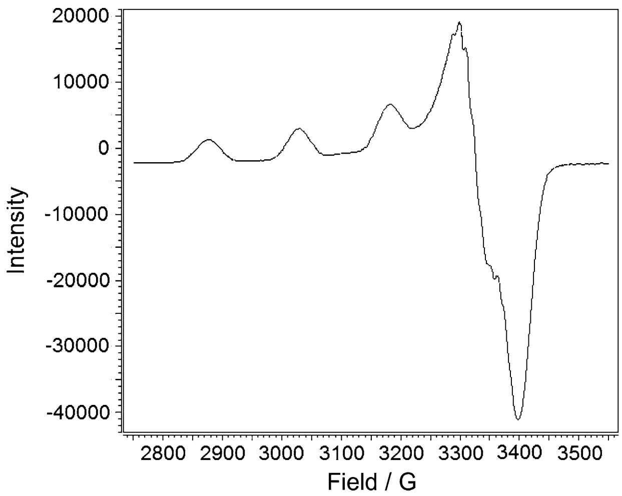

Fig. 3 EPR analysis of Cu(II) complex **8** at 115 K in MeOH

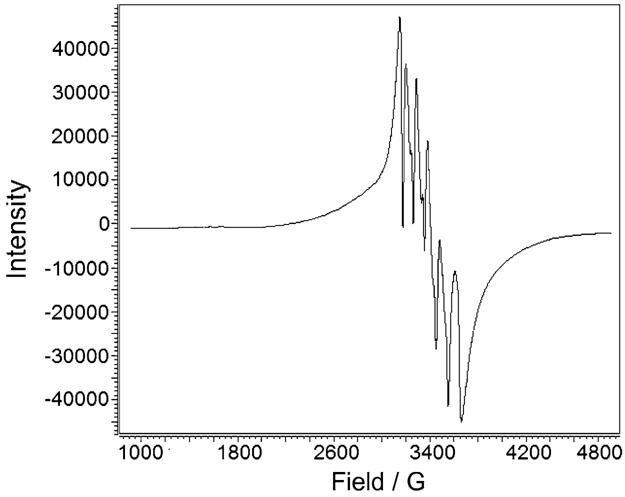

Fig. 4 EPR analysis of Mn(II) complex **10** at 115 K in DMSO

are assigned to the d ↔ d transition [71] and the position of these bands indicates that the chelate ligand coordinated to the central metal ion in a square-planar structure. The broad band observed at 351 nm in the electronic spectrum of the Cu(II) complex was assigned to the $^2E_g \rightarrow {}^2T_{2g}$ transition which is consistent with octahedral geometry including the two acetate anions [72].

*TGA analysis of complexes **8–10***

The thermogravimetric (TGA) analyses of **8–10** were performed using air as the gas carrier. The complexes were heated at rate of 10.0 °C per min from 30.0 to 600.0 °C. The thermogram of the studied complexes shows that the complexes decomposed in three successive steps. This is attributed to the loss of solvent molecules, acetate ions, and bis(diphenylphosphino) groups of the complexes for the first, second, and third steps, respectively.

In the thermogram of the complexes, the first endothermic weight loss of **8** was observed between 150 and 180 °C and ascribed to the loss of one coordinated water molecule. The experimental mass loss value ($\Delta m_{\mathrm{rel}} = 1.90\ \%$) approximately agrees with the expected one ($\Delta m_{\mathrm{rel}} = 1.08\ \%$) in complex **8**. In complex **9**, the methanol molecule was lost at 100–120 °C with an observed mass loss value ($\Delta m_{\mathrm{rel}} = 3.06\ \%$) which agrees with the expected value ($\Delta m_{\mathrm{rel}} = 3.48\ \%$). This suggests that the methanol molecule was part of the lattice structure in complex **9**. The complexes **8** and **9** did not show any weight loss until a temperature of 300 °C after which they decomposed without melting. Complex **9** underwent exothermic loss at 250 °C ($\Delta m_{\mathrm{rel}} = 9.05\ \%$) which corresponds to one acetate group as expected theoretically ($\Delta m_{\mathrm{rel}} = 9.90\ \%$). But in complex **8**, exothermic loss occurred at 350 °C with $\Delta m_{\mathrm{rel}} = 33.58\ \%$, which is due to the loss of the two acetate groups and two phenyl groups of the bis(diphenylphosphino) groups ($\Delta m_{\mathrm{rel}} = 33.60\ \%$). In both **8** and **9**, the acetate group was assumed to be lost as acetic acid. The third part of the TGA decomposition of **8** and **9** is attributed to the loss of two diphenylphosphino groups and the central metal ion.

The second endothermic weight loss of complex **10** in the thermogram was observed between 250 and 300 °C owing to the loss of the coordinated methanol molecule, two acetate anions, and two phenyl groups of the bis(diphenylphosphino) group. The experimental mass loss value ($\Delta m_{\mathrm{rel}} = 33.91\ \%$) approximately agrees with the expected one ($\Delta m_{\mathrm{rel}} = 35.07\ \%$). Then the third endothermic weight loss of complex **10** was observed between 450 and 500 °C which corresponds to the loss of the two additional phenyl groups of the bis(diphenylphosphino) groups. The experimental mass loss value ($\Delta m_{\mathrm{rel}} = 54.93\ \%$) approximately agrees with the expected one ($\Delta m_{\mathrm{rel}} = 52.84\ \%$).

*Activation energy and pH stability of complexes **8–10***

The activation energy (E/kJ mol^{-1}) of the studied complexes **8–10** could be calculated from Eq. (1) as shown in Fig. 5. Equation (1) shows the linear relation between log s (observed conductance) versus $1/T$ (the reciprocal of temperature from 298 to 333 K) [73]. The observed conductance of the current complexes is tabulated at various temperatures (from 25 to 60 °C) in the Supplementary Material.

$$s = s^0 \exp(-E/2kT) \tag{1}$$

where s is the observed conductance of the complex solution, s^0 is the specific conductance (a constant value), and E is the activation energy of the charged complex ions in the solution. The observed conductivities follow the order **10** < **9** < **8** (Table 2). This order agrees with the effect of the type of central metal ion and its geometry in complexation with the title ligands on the conductivity of the complexes for all applied temperatures [74]. The activation energies of the charged complex ions decrease in the following direction **9** < **10** < **8**, which parallels the increased conductivities of these complexes.

The pH stability was tested using universal buffer solutions [74] added to an ethanolic solution of **8**, **9**, or **10**, followed by measuring the absorbance at $\lambda_{\max}$ at room temperature. The investigated complex ions are highly stable within a wide range of pHs, from ca. 4.5 to 7.5 (see Supplementary Material). The tested solutions of **8–10** in the aforementioned pH range maintain their colors for more than 3 days without fading. This observation shows the extent of the stability of our studied complexes in that pH range. But outside that range the colors of the complex ions fade at once.

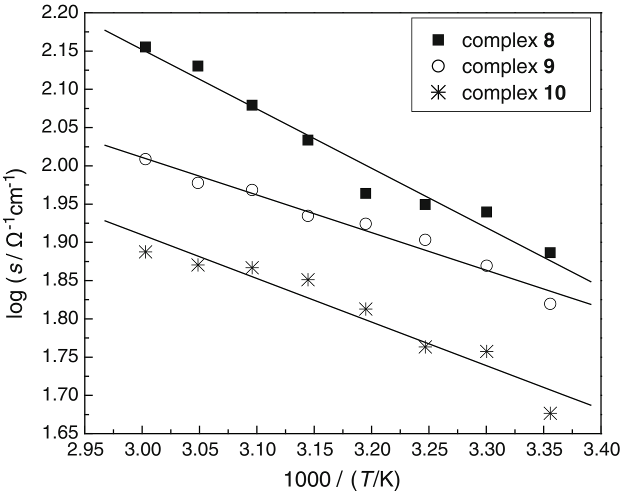

Fig. 5 Plot of logarithm of the observed conductivity of complexes **8–10** at ca. 2 × 10^{-4} mol dm^{-3} versus 1,000/T

Experimental

Reactions with moisture- or air-sensitive compounds were conducted in dried and deoxygenated solvents under a nitrogen atmosphere using Schlenk techniques, carried out with magnetic stirring, and held at the chosen temperature by immersion in a thermostatted oil bath. Hydrazine monohydrate, diethyloxalate, diethylomalonate, methyl diethylomalonate, ethyl diethylomalonate, chlorodiphenylphosphine, 1,2-dibromobenzene, *n*-BuLi (2.5 M in hexane), palladium acetate, copper acetate monohydrate, and manganese acetate dihydrate were used as received from commercial suppliers (Sigma-Aldrich, Merck, and Acros).

Oxalyl, malonyl, methyl-malonyl, and ethyl-malonyl dihydrazides (**4** and **5a**–**5c**) were synthesized by the literature methods [48, 54]. The oxalyl, malonyl, methyl-malonyl, and ethyl-malonyl dicarboxylic acid esters reacted directly with hydrazine monohydrate in ethanolic solution by refluxing or by stirring at room temperature to give white precipitates of the corresponding dihydrazides. *o*-(Diphenylphosphino)benyaldehyde (**3**) was prepared as reported before [53].

Some analyses of the synthesized compounds were carried out in collaboration with Prof. Dr. Rinaldo Poli labs, Inorganic Chemistry, Laboratoire de Chimie de Coordination (LCC), UPR CNRS 8241 205, Route de Narbonne, 31077 Toulouse Cedex 4, France (NMR, EA, and PR analyses). NMR spectra were recorded at 25 °C on a multinuclear FT-NMR spectrometer Bruker ARX300 and ARX250 at 300 (^{1}H), 75 (^{13}C), and 121 (^{31}P) MHz. The ^{1}H, ^{13}C, and ^{31}P chemical shifts are given in ppm relative to Me_4Si and H_3PO_4 (85 %), respectively, as external standards. Coupling constants refer to J_{HH} in ^{1}H and J_{PC} in ^{13}C NMR unless denoted otherwise. Splitting patterns for larger and smaller coupling constants are given in the same order as the J values. Mass spectra were recorded on a Finnigan MAT system 8200 spectrometer, equipped with a 3-T superconducting magnet with ESI. Elemental analyses (C, H, N, S) were conducted using a CHNS-932 analyzer from LECO using standard conditions; their results were found to be in good agreement with calculated values (±0.4 %). Conductivity measurements were carried out using Jenway conductivity meter model 4320, using an epoxy-bodied conductivity cell (two electrodes, shiny) with cell constant calibration (from 0.01 to 19.99) at 298 K, which was controlled by an ultrathermostat (HAAKE model F3-k) within ±0.2 °C. The electronic spectra of ligands **6** and **7a**–**7c** and the complexes **8**–**10** were measured using 10-mm silica cells in the thermostatted cell holder of a Jasco UV–Vis spectrophotometer (model V-530). The thermostatted cell holder was fitted with an ultrathermostat water circulator (HAAKE model F3-k). pH values were checked using a Metrohm 695 pH/ion meter to ±0.005 units with temperature control using an ultrathermostat (HAAKE model F3-k) within ±0.2 °C.

General procedure for the synthesis of oxalic and (substituted) malonic acid dihydrazides

Under a nitrogen atmosphere in a two-necked round-bottomed flask equipped with a dropping funnel 5 cm^{3} of ethanolic solution of *o*-(diphenylphosphino)benzaldehyde (**3**) was poured into 5 cm^{3} of an ethanolic solution of oxalyl, malonyl, methyl-malonyl, or ethyl-malonyl dihydrazide and anhydrous sodium acetate or triethylamine (TEA). The reaction mixture was refluxed for a period of time controlled by TLC. A white precipitate was formed which was collected by filtration, washed many times with EtOH, and purified by column chromatography.

Oxalic acid 1,2-bis[2-[2-(diphenylphosphino)phenylmethylene]hydrazide] (**6**, $C_{40}H_{32}N_4O_2P_2$)
Reaction of 0.38 g **3** (1.30 mmol) with 0.077 g **4** (0.65 mmol) and 0.10 g anhydrous sodium acetate (1.30 mmol) or 0.09 cm^{3} TEA (1.30 mmol) under reflux for 2 h. Purification of the final product by column chromatography was carried out using 40 % ethyl acetate/60 % *n*-hexane to afford 0.39 g (91 %) of **6**. M.p.: 248 °C; ^{1}H NMR (300 MHz, $CDCl_3$): $\delta = 6.95$ (dd, 2H, $^{3}J = 4.5$, $^{4}J = 0.9$ Hz), 7.23–7.45 (m, 24 H), 8.24 (dddd, 2H, $^{3}J = 4.2$, 3.9, $^{4}J = 1.2$, 0.9 Hz), 8.99 (d, CH=N, $^{4}J_{PH} = 5.7$ Hz), 10.23 (s, br, 2 NH) ppm; ^{13}C NMR (75 MHz, $CDCl_3$): $\delta = 127.3$, 128.7, 128.8, 129.1, 129.2, 131.1, 133.7, 134.1, 135.4, 135.6, 136.4, 136.7, 137.6, 137.9, 149.6, 150.1, 155.0 ppm; ^{31}P NMR (121 MHz, $CDCl_3$): $\delta = -11.67$ ($J_{PP} = 19.6$ Hz) ppm; IR (KBr): $\bar{\nu} = 3{,}454.0$ (NH), 3,059.5, 750.4 (C=CH aromatic), 1,978.2 (N–C=O), 1,687.0 (C=O), 1,505.6 (C=N, amide), 1,439.1 (C–N) cm^{-1}; MS (ESI MS CI+, DCI/CH_4): *m*/*z* = 662.

Malonic acid 1,3-bis[2-[2-(diphenylphosphino)phenylmethylene]hydrazide] (**7a**, $C_{41}H_{34}N_4O_2P_2$)
Reaction of 0.40 g **3** (1.37 mmol) with 0.09 g **5a** (0.68 mmol) and 0.11 g anhydrous sodium acetate (1.37 mmol) or 0.10 cm^{3} TEA (1.37 mmol) under reflux overnight. Purification of the final product by column chromatography was carried out using 40 % ethyl acetate/60 % *n*-hexane to afford 0.43 g (93 %) of **7a**. M.p.: 198 °C; ^{1}H NMR (300 MHz, $CDCl_3$): $\delta = 3.97$ (s, 2H, CH_2), 6.88–6.93 (m, 2 H), 7.21–7.33 (m, diphenyl, overlapped with solvent peak), 7.91 (dd, $^{3}J = 4.2$, 3.9 Hz), 8.46 (t, 2H, overlapped with the carbonyl–enol form, $^{3}J = 5.1$, 3.3 Hz), 9.03 (s, CH=N) ppm; ^{1}H NMR signals which could be distinguished for the dicarbonyl

form are 3.80 (s, 2H, CH$_2$), 8.21 (dd, $^3J = 4.5$, 3.6 Hz), 8.87 (t, $^3J = 5.7$ Hz), 10.70 (br s, 2 NH) ppm; ^{1}H NMR signals which could be distinguished for the carbonyl–enol form are 3.31 (s, 2H, CH$_2$), 8.00 (dd, $^3J = 4.4$, 3.7 Hz), 9.10 (s, CH=N), 10.58 (br s, 1 NH) ppm; from the integration factor, the ratio of dienol to dicarbonyl to carbonyl–enol form is 1.8:1.0:0.8; ^{13}C NMR (75 MHz, CDCl$_3$): $\delta = 29.7$ (CH$_2$), 38.4 (CH$_2$), 39.7 (CH$_2$), 126.8 (CH), 127.2 (CH), 128.6 (CH), 129.0 (CH), 129.1 (CH), 129.9 (CH), 130.3 (CH), 130.4 (CH), 133.7 (CH), 133.9 (CH), 134.0 (CH), 135.8 (C$_q$), 136.0 (C$_q$), 136.5 (C$_q$), 136.8 (C$_q$), 137.0 (C$_q$), 142.3 (d, CH, $J = 24.5$ Hz), 144.2 (d, CH, $J = 20.5$ Hz), 146.5 (d, CH, $J = 28.4$ Hz), 162.1 (C$_q$, C=O), 169.2 (C$_q$, C=O), 169.8 (C$_q$, C=O) ppm; ^{31}P NMR (121 MHz, CDCl$_3$): $\delta = -16.55$, -16.08, -14.79, -14.26 ppm; IR (KBr): $\bar{\nu} = 3{,}463.6$ (OH), 3,421.2 (NH), 3,090, 742.7 (C=CH, aromatic), 2,928.3, 694.5 (CH, aliphatic), 1,660.9 (C=O), 1,571.3 (C=N), 1,390.8 cm^{-1} (C=N, tautomer), 1,369.2 (C–N) cm^{-1}; MS (EI+ 30 eV): $m/z = 677$ [M$^+$].

2-Methylmalonic acid 1,3-bis[2-[2-(diphenylphosphino)-phenylmethylene]hydrazide] (**7b**, C$_{42}$H$_{36}$N$_4$O$_2$P$_2$)

Reaction of 0.40 g **3** (1.37 mmol) with 0.10 g **5b** (0.68 mmol) and 0.11 g anhydrous sodium acetate (1.37 mmol) or 0.10 cm^3 TEA (1.37 mmol) under reflux overnight. Purification of the final product by column chromatography was carried out using 40 % ethyl acetate/60 % *n*-hexane to afford 0.40 g (85 %) of **7b**. M.p.: 174 °C; ^{1}H NMR (300 MHz, CDCl$_3$): $\delta = 1.46$ (t, 3H, CH$_3$, $^3J = 7.2$ Hz), 4.55 (q, 1H, CH, $^3J = 7.5$, 7.2 Hz), 6.89–7.00 (m, 2 H), 7.13–7.47 (m, 10H, diphenyl), 7.96 (m, 2H, $^3J = 4.0$, 3.4 Hz), 8.44 (d, $^3J = 5.2$ Hz), 8.59 ppm (s, CH=N); ^{1}H NMR signals which could be distinguished for the dicarbonyl form are 1.61 (br, 3H, CH$_3$), 4.23 (q, 1H, CH, $^3J = 7.2$ Hz), 8.14 (m), 9.22 (d, $^3J = 4.7$ Hz), 8.68 (s, CH=N), 10.38 (br s, 2 NH) ppm; ^{1}H NMR signals which could be distinguished for the carbonyl–enol form are 8.17 (m), 8.36 (d, $^3J = 4.2$ Hz), 8.89 (d, $^3J = 5.5$ Hz) ppm; ^{13}C NMR (75 MHz, DMSO-*d*$_6$): $\delta = 13.1$ (CH$_3$), 14.2 (CH$_3$), 45.2 (CH), 126.4 (CH), 126.6 (CH), 126.7 (CH), 129.1 (CH), 129.3 (CH), 129.4 (CH), 129.6 (CH), 130.0 (CH), 133.6 (CH), 133.8 (CH), 133.9 (CH), 134.1 (CH), 135.8 (C$_q$), 136.1 (C$_q$), 136.1 (C$_q$), 136.2 (C$_q$), 136.4 (C$_q$), 138.3 (d, C$_q$, $J = 20.7$ Hz), 139.8 (d, CH, $J = 28.0$ Hz), 168.2 (C$_q$, C=O), 171.5 (C$_q$, C=O), 173.1 (C$_q$, C=O) ppm; ^{31}P NMR (121 MHz, DMSO-*d*$_6$): $\delta = -18.31$, -17.28, -16.73, -16.00 ppm; IR (KBr): $\bar{\nu} = 3{,}460.0$ (br, OH and NH), 3,055.6, 746.5 (C=CH, phenyl), 2,929.3, 695.4 (CH, aliphatic), 2,365.0 (weak, N–C=O), 1,680.2 (C=O), 1,560.6 (C=N, amide), 1,452.6 (C=N, tautomer), 1,366.7 (C–N) cm^{-1}; MS (ESI MS CI+, DCI/CH$_4$): $m/z = 691$ [M$^+$].

2-Ethylmalonic acid 1,3-bis[2-[2-(diphenylphosphino)phenylmethylene]hydrazide] (**7c**, C$_{43}$H$_{38}$N$_4$O$_2$P$_2$)

Reaction of 0.40 g **3** (1.37 mmol) with 0.11 g **5c** (0.68 mmol) and 0.11 g anhydrous sodium acetate (1.37 mmol) or 0.10 cm^3 TEA (1.37 mmol) under reflux overnight. Purification of the final product was by column chromatography carried out using 30 % ethyl acetate/70 % *n*-hexane to afford 0.36 g (75 %) of **7c**. M.p.: 170 °C; ^{1}H NMR (300 MHz, CDCl$_3$): $\delta = 0.94$ (t, 3H, CH$_3$, $^3J = 7.5$, 7.2 Hz), 2.04 (m, 2H, CH$_2$), 4.24 (t, 1H, CH, $^3J = 7.2$ Hz), 6.89–6.97 (m, 2 H), 7.09–7.45 (m, diphenyl, overlapped with solvent peak), 8.00 (dddd, 2H, $^3J = 4.2$, 3.7, $^4J = 1.0$, 0.8 Hz), 8.23 (ddd, $^3J = 3.7$, $^4J = 1.0$ Hz), 8.48 (d, $^3J = 5.5$ Hz), 8.63 (s, CH=N), 8.88 (d, $^3J = 5.5$ Hz) ppm; ^{1}H NMR signals which could be distinguished for the dicarbonyl form are 1.07 (t, 3H, CH$_3$, $^3J = 7.5$ Hz), 4.65 (t, 1H, CH, $^3J = 7.2$, 7.0 Hz), 7.94 (dddd, 2H, $^3J = 4.2$, 3.7, $^4J = 1.0$, 0.5 Hz), 8.15 (ddd, $^3J = 4.0$, $^4J = 1.2$ Hz), 8.38 (d, $^3J = 4.5$ Hz), 8.69 (s, CH=N), 9.22 (d, $^3J = 4.5$ Hz), 10.38 (br s, 2 NH) ppm; ^{1}H NMR signals which could be distinguished for the carbonyl–enol form are 0.99 (t, 3H, CH$_3$, $^3J = 7.2$ Hz), 8.85 (d, $^3J = 5.7$ Hz), 10.16 (br s, 2 NH) ppm; ^{13}C NMR (75 MHz, DMSO-*d*$_6$): $\delta = 11.4$ (CH$_3$), 47.2 (CH), 49.4 (CH), 126.2 (CH), 126.3 (CH), 127.2 (CH), 128.5 (CH), 128.7 (CH), 129.1 (CH), 130.7 (CH), 133.7 (CH), 133.9 (CH), 134.0 (CH), 135.8 (C$_q$), 141.1 (CH), 171.2 (C$_q$, C=O) ppm; ^{31}P NMR (121 MHz, CDCl$_3$): $\delta = -16.81$, -16.66, -15.99, -14.89, -13.42 ppm; MS (EI+ 30 eV): $m/z = 705$ ([M+1]$^+$); HRMS: calcd 705.2504, found 705.2548.

[Oxalic acid 1,2-bis[2-[2-(diphenylphosphino)phenylmethylene]hydrazide]]copper(II) acetate·H$_2$O
(**8**, C$_{44}$H$_{40}$CuN$_4$O$_7$P$_2$)

Under nitrogen in a two-necked round-bottomed flask 5 cm^3 of a methanolic solution of 0.05 g Cu(CH$_3$COO)$_2$·H$_2$O (0.25 mmol) was added dropwise to 5 cm^3 of a methanolic solution of 0.17 g **6** (0.25 mmol). The color of the reaction mixture changed to pale green just after addition of the Cu^{2+} solution. The reaction mixture was stirred at room temperature for 3 h to afford an olive-brown precipitate. The precipitate was filtrated and washed many times with ethanol and ether and then dried in vacuo. The complex was recrystallized from ethanol to afford 0.14 g (64 %) of **8**. M.p.: >300 °C (dec.); IR (KBr): $\bar{\nu} = 3{,}424.1$ (NH), 3,060.0, 749.4 (C=C–H, aromatic), 2,926.4, 694.5 (C–H aliphatic), 2,364.1 (N–C=O), 1,698.5 (C=O), 1,636.8 (C=N, amide), 1,495.0 (C=N, tautomer), 1,376.4 (C–N) cm^{-1}; MS (ESI in CH$_3$Cl/MeOH–CH$_3$COO$^-$): $m/z = 725$ [M$^+$].

[Oxalic acid 1,2-bis[2-[2-(diphenylphosphino)phenylmethylene]hydrazide]]palladium(II) acetate·MeOH
(**9**, $C_{45}H_{42}N_4O_7P_2Pd$)

Under nitrogen in a two-necked round-bottomed flask 5 cm^3 of a methanolic solution of 0.033 g $Pd(CH_3COO)_2$ (0.15 mmol) was added dropwise to 5 cm^3 of a methanolic solution of 0.10 g **6** (0.15 mmol). The reaction mixture was kept under stirring at room temperature for 4 h to afford a brown precipitate. The precipitate was filtrated and washed many times with ethanol and ether and then dried in vacuo. The complex was recrystallized from methanol to afford 0.14 g (60 %) of **9**. M.p.: >300 °C; ^{1}H NMR (300 MHz, $CDCl_3$): $\delta = 1.84$ (s, 3H, CH_3, acetate), 5.97 (br s, 1H, CH_3, MeOH), 6.97 (m, 4 H), 7.26–7.61 (m, 10H, overlapped with solvent peak), 7.51 (t, 1H, $^3J = 7.7$ Hz), 9.01 (d, 1H, CH=N, $^3J = 11.2$ Hz) ppm; ^{13}C NMR (75 MHz, $CDCl_3$): $\delta = 22.0$ (CH_3, acetate), 123.3, 123.8, 124.2, 127.5, 128.7, 128.9, 130.9, 131.8, 132.5, 133.4, 133.6, 136.1, 156.0, 169.0, 175.5 (C=O of acetate) ppm; ^{31}P NMR (101.25 MHz, $CDCl_3$): $\delta = 31.47$ ppm (contaminated with very small signals of the reactant, 16.1, 33.16, 35.68 ppm); IR (KBr): $\bar{\nu} = 3{,}421.2$ (br, interfering of MeOH and NH), 3,053.7, 745.6 (C=C–H, aromatic), 2,938.9, 693.5 (C–H aliphatic), 1,685.0 (C=O), 1,523.0 (C=N, amide), 1,431.4 (C=N, tautomer), 1,359.7 (C–N) cm^{-1}; MS (ESI in MeOH): $m/z = 886$ [M$^+$].

[Oxalic acid 1,2-bis[2-[2-(diphenylphosphino)phenylmethylene]hydrazide]]manganese(II) acetate·MeOH
(**10**, $C_{45}H_{42}MnN_4O_7P_2$)

Under nitrogen in a two-necked round-bottomed flask 5 cm^3 of a methanolic solution of 0.05 g $Mn(CH_3COO)_2\cdot 2H_2O$ (0.23 mmol) was added dropwise to 5 cm^3 of a methanolic solution of 0.15 g **6** (0.23 mmol). The reaction mixture was kept under stirring at room temperature for 4 h to afford a brown precipitate. The precipitate was filtrated and washed many times with ethanol and ether and then dried in vacuo. The complex was recrystallized from methanol to afford 0.045 g (69 %) of **10**. M.p.: >300 °C (dec.); IR (KBr): $\bar{\nu} = 3{,}420.2$ (br, interfering of MeOH and NH), 3,056.0, 716.6 (C=C–H, aromatic), 2,929.3 (C–H aliphatic), 1,564.5 (strong br, C=O, C=N, amide), 1,423.6 (C=N, tautomer), 1,312.7 (C–N) cm^{-1}; MS (ESI in MeOH): $m/z = 835$ [M$^+$].

Acknowledgments The authors greatly thank Prof. Dr. Rinaldo Poli, Laboratoire de Chimie de Coordination (LCC), UPR CNRS 8241 205, Route de Narbonne, 31077 Toulouse Cedex 4, France, for his continued and precious advice and encouragement to produce this work.

References

1. Bharti N, Maurya MR, Naqvi F, Bhattacharya A, Bhattacharya S, Azam A (2000) Eur J Med Chem 35:481
2. Sridhar SK, Pandeya SN, Stables JP, Ramesh A (2002) Eur J Pharm Sci 16:129
3. Louie AY, Meade TJ (1999) Chem Rev 99:2711
4. Lal RA, Basumatary D, Adhikari S, Kumar A (2008) Spectrochim Acta A 69:706
5. Van Veggel FCJM, Bos M, Harkema S, Van de Bovenkamp H, Verboom W, Reedijk J, Reinhoudt DN (1991) J Org Chem 56:225
6. Lal K, Gupta SP, Sahni SK (1986) Polyhedron 5:1499
7. Lal RA, Thapa RK, Das S (1987) Inorg Chim Acta 132:129
8. Vigato PA, Tamburini J, Fenton DE (1990) Coord Chem Rev 106:25
9. Lal RA, Adhikari S, Kumar A, Chakraborty J (2001) Synth React Inorg Met Org Chem 31:65
10. Salavati-Niasari M, Sobhani A (2008) J Mol Catal A 285:58
11. DiRenzo GM, White PS, Brookhart M (1996) J Am Chem Soc 118:6225
12. De Felice V, Cucciolito ME, De Renzi A, Ruffo F, Tesauro D (1995) J Organomet Chem 493:1
13. Britovsek GJP, Keim W, Mecking S, Sainz D, Wagner T (1993) Chem Commun 1632–1634
14. Garralda MA, Hernandez R, Ibarlucea L, Pinilla E, Torres MR (2003) Organometallics 22:3600
15. Yeh W-Y, Lin C-S, Peng S-M, Lee G-H (2004) Organometallics 23:917
16. Newkome GR (1993) Chem Rev 93:2067
17. Nardelli M, Pelizzi C, Pelizzi G, Tarasconi P (1985) J Chem Soc Dalton Trans 321–415
18. Cingolani A, Effendy, Pellei M, Pettinari C, Santini C, Skelton BW, White AH (2002) Inorg Chem 41:6633
19. Enders D, Gielena H, Raabea G, Runsink J, Teles JH (1996) Chem Ber 129:483
20. Cingolani A, Effendy, Martini D, Pettinari C, Skelton BW, White AH (2006) Inorg Chim Acta 359:2183
21. Bader A, Lindner E (1991) Coord Chem Rev 108:27
22. Del Zotto A, Baratta W, Ballico M, Herdtweck E, Rigo P (2007) Organometallics 26:5636
23. Tollabi M, Framery E, Goux-Henry C, Sinou D (2003) Tetrahedron Asymmetry 14:3329
24. Konovets A, Glegola K, Penciu A, Framery E, Jubault P, Goux-Henry C, Pietrusiewicz KM, Quirion JC, Sinou D (2005) Tetrahedron Asymmetry 16:3183
25. Johannesen SA, Glegoła K, Sinou D, Framery E, Skrydstrup T (2007) Tetrahedron Lett 48:3569
26. Best J, Wilson JM, Adams H, Gonsalvi L, Peruzzini M, Haynes A (2007) Organometallics 26:1965
27. Ramırez P, Contreras R, Valderrama M, Carmona D, Lahoz FJ, Balana AI (2008) J Organomet Chem 693:349
28. Biradar DB, Gau H-M (2008) Tetrahedron Asymmetry 19:733
29. Nakano H, Takahashi K, Okuyama Y, Senoo C, Tsugawa N, Suzuki Y, Fujita R, Sasaki K, Kabuto C (2004) J Org Chem 69:7092
30. Wencel J, Laurent I, Toupet L, Crevisy C, Mauduit M (2010) Organometallics 29:1530
31. del Campo O, Carbayo A, Cuevas JV, García-Herbosa G, Muñoz A (2009) Eur J Inorg Chem 2254–2260
32. Sui-Seng C, Haque FN, Hadzovic A, Pütz A-M, Reuss V, Meyer N, Lough AJ, De Iuliis MZ, Morris RH (2009) Inorg Chem 48:735
33. Meyer N, Lough AJ, Morris RH (2009) Chem Eur J 15:5605
34. Mikhailine A, Lough AJ, Morris RH (2009) J Am Chem Soc 131:1394
35. Sui-Seng C, Freutel F, Lough AJ, Morris RH (2008) Angew Chem Int Ed 47:940
36. Downing JH, Smith MB (2003) In: Lever ABP (ed) Comprehensive coordination chemistry II, vol 1. Elsevier, Oxford, p 253

37. McAuliffe CA (1987) In: Wilkinson G, Gillard RD, McCleverty JA (eds) Comprehensive coordination chemistry, vol 2. Pergamon, Oxford, p 990
38. Köhl O (2005) Coord Chem Rev 249:693
39. Tolman CA (1977) Chem Rev 77:313
40. Tang W, Zhang X (2003) Chem Rev 103:3029
41. Crepy KVL, Imamoto T (2003) Top Curr Chem 229:1
42. Guiry PJ, Saunders CP (2004) Adv Synth Catal 346:497
43. Markovskii LN, Romanenko VD (1989) Tetrahedron 45:6019
44. Jiang J-J, Huang J, Wang D, Zhao M-X, Wang F-J, Shi M (2010) Tetrahedron Asymmetry 21:794
45. Jiang J-J, Wang D, Wang WF, Yuan Z-L, Zhao M-X, Wang F-J, Shi M (2010) Tetrahedron Asymmetry 21:2050
46. Jacobsen EN, Pfaltz A, Yamamoto H (1999) Comprehensive asymmetric catalysis. Springer, Berlin
47. Genet JP, Greck C, Lavergne D (2000) In: Ricci A (ed) Modern amination methods. Wiley, Weinheim, Chap. 3
48. Hadjoudis E, Mavridis IM (2004) Chem Soc Rev 22:579
49. Filarowski A (2005) J Phys Org Chem 18:686
50. Jungreis E, Thabet S (1969) Analytical application of Schiff bases. In: Flasha HA, Barnard AJ (eds) Chelates in analytical chemistry. Marcel Dekker, New York
51. Galic N, Cimerman Z, Tomisic V (1997) Anal Chim Acta 343:135
52. Salavati-Niasari M (2006) Microporous Mesoporous Mater 92:173
53. Luo X, Zhang H, Duan H, Liu Q, Zhu L, Zhang T, Lei A (2007) Org Lett 9:4571
54. Lal R, Mukherjee LM, Siva AN, Pal A, Adhikarik S, Narang KK, Singh MK (1993) Polyhedron 12:2351
55. Zhang C, Rheinwald G, Lozan V, Wu B, Lassahn P-G, Lang H, Janiak C (2002) Z Anorg Allg Chem 628:1259
56. Rozwadowski Z, Dziembowska T, Schroeder G, Brzezinski B (1998) J Mol Struct 444:221
57. Szlyk E, Surdykowski A, Barwiolek M, Larsen E (2002) Polyhedron 21:2711
58. Reichardt C (2003) Solvents and solvent effects in organic chemistry. Wiley, Weinheim
59. Stewart JJP (1990) J Comput Aided Mol Des 4:1
60. Dewar MJS, Healy EF, Stewart JJP (1984) J Chem Soc Faraday Trans 2(80):227
61. Ranford JD, Vittal JJ, Wang YM (1998) Inorg Chem 37:1226
62. Job P (1928) Ann Chim Phys 9:113
63. Fouda MFR, Abd-el-zaher MM, Shadofa MME, El Saied FA, Ayad MI, El Tabl AS (2008) Transit Met Chem 33:219
64. Chandra S, Kuar U (2005) Spectrochim Acta A 61:219
65. Gudasi KB, Patil SA, Vadavi RS, Shenoy RV (2006) Transit Met Chem 31:586
66. Hathway BJ, Billing DE (1966) Coord Chem Rev 5:143
67. Raman N, Rabichandran S, Thangaraja DE (2004) J Chem Sci 116:215
68. Rajan R, Rajaram R, Nair BU, Ramsami T, Mandal SK (1996) J Chem Soc Dalton Trans 2019–2021
69. Drago RS (1977) Physical methods in chemistry. Saunders, St. Louis, p 530
70. Kim Bong BI, Miyake C, Imoto S (1975) J Inorg Nucl Chem 37:963
71. Bertini I, Canti G, Grassi R, Scozzafava A (1980) Inorg Chem 19:2198
72. Dunn TM (1960) The visible and ultraviolet spectra of complex compounds in modern coordination chemistry. Interscience, New York
73. Ogata Y, Takagi Y (1958) J Chem Soc Dalton Trans 80:3591
74. Shaker AM, Adam MS (2003) Synth React Inorg Met Org Chem 33:1081